THE JOURNAL OF PHYSICAL CHEMISTRY A LETTERS

2008, *112,* 2511−2514
Published on Web 02/15/2008

Excited State Hydrogen Bond Dynamics: Coumarin 102 in Acetonitrile−Water Binary Mixtures

Nathan P. Wells, Matthew J. McGrath, J. Ilja Siepmann, David F. Underwood, and David A. Blank*

Department of Chemistry, University of Minnesota, 207 Pleasant Street SE, Minneapolis, Minnesota 55455

Received: November 14, 2007; In Final Form: December 20, 2007

The time dependent change in the intermolecular response of solvent molecules following photoexcitation of Coumarin 102 (C102) has been measured in acetonitrile−water binary mixtures. Experiments were performed on mixtures of composition $x_{CH_3CN} = 0.25$, 0.50, 0.75, and 1.00. At low water concentrations ($x_{H_2O} \leq 0.25$) the solvent response is consistent with previous measurements probing dipolar solvation. With increasing water concentration ($x_{H_2O} \geq 0.50$) an additional response is found subsequent to dipolar solvation, exhibited as a rapid gain in the solvent's polarizability on a ∼250 fs time scale. Monte Carlo simulations of the C102: binary mixture system were performed to quantify the number of hydrogen-bonding interactions between C102 and water. These simulations indicate that the probability of the C102 solute being hydrogen bound with two water molecules, both as donors at the carbonyl site, increases in a correlated fashion with the amplitude of the additional response in the measurements. We conclude that excitation of C102 simultaneously weakens and strengthens hydrogen bonding in complexes with two inequivalently bound waters.

The solvent can play an integral role in liquid-phase chemical transformations. Solvent environments can give rise to static effects such as shifting the relative energies of reactants and products, as well as changing the barrier height at the transition state.[1] The solvent dynamics can also be important factors in understanding reactions in solution. In charge transfer reactions reorganization of the surrounding solvent is often cast as the primary reaction coordinate.[2] In addition to electrostatic and dispersive solvent−solute interactions, hydrogen bonding can have a profound effect on solute dynamics. Elsaesser and co-workers, and Yoshihara and co-workers, have reported significant changes in the hydrogen bonding between the laser dye Coumarin 102 (C102) and various hydrogen bond donors following photoexcitation of C102 in solution.[3−7] The structure of C102 is shown in Figure 1. The authors have assigned transient absorption behavior of the IR active vibrations at the hydrogen-bonding site, and of the electronic transition in C102, to cleavage of the hydrogen bond at the carbonyl in less than 200 fs. Although the spectroscopic evidence is compelling, it appears to be at odds with calculations of electrostatic changes on the carbonyl and more recent time-dependent density functional theory calculations that indicate an increase in the hydrogen bond strength upon excitation of the C102 in isolated (gas phase) complexes.[4,8,9]

In this Letter we report ultrafast spectroscopic measurements on C102 in acetonitrile−water binary mixtures. Using a technique recently developed in our laboratory, we measured time dependent changes in the intermolecular solvent response following resonant excitation of C102.[10,11] In all of the solutions we observe a change in the response due primarily to an increase in the solvent−solute electrostatic interaction that follows a large increase in the C102 dipole moment. However, for solutions with $x_{H_2O} \geq 0.5$ we find an additional response component, of opposite sign, that is roughly proportional to x_{H_2O} in amplitude. This additional change takes place on similar time scales to the previously assigned ultrafast hydrogen bond cleavage in the excited state between C102 and nonaqueous donors.[3−7] Monte Carlo simulations are presented that demonstrate a correlation between our observations and the probability of two hydrogen-bonded waters, both as donors at the carbonyl site on C102, as a function of composition. Considered together with the experimental results, a model for the hydrogen-bonding dynamics between C102 and water after C102 excitation is proposed that accommodates both hydrogen bond strengthening and cleavage.

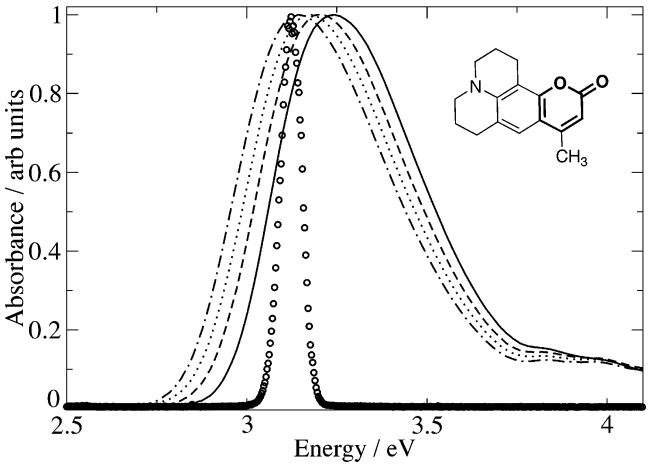

Figure 1. C102 absorption spectra. The data for $x_{CH_3CN} = 1.00$, 0.75, 0.50, and 0.25 are given as the solid, dashed, dotted, and dashed−dot lines respectively. The circles are the spectrum of the laser pulse used for excitation of C102.

* Corresponding author. E-mail: blank@umn.edu.

10.1021/jp710889t CCC: $40.75

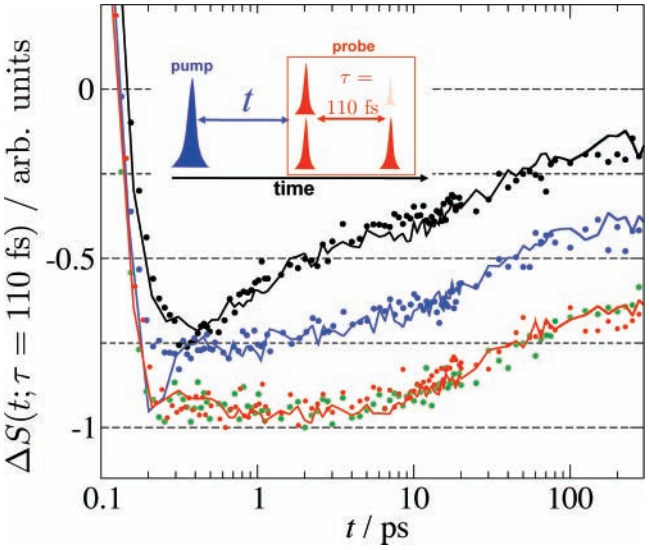

Figure 2. Change in the third-order Raman response. From bottom to top: green, $x_{CH_3CN} = 1.00$; red, $x_{CH_3CN} = 0.75$; blue, $x_{CH_3CN} = 0.50$; black, $x_{CH_3CN} = 0.25$. The solid lines represent the fits. Note that the noise on the fits originates from direct inclusion in the fits of background measurements on identical solutions without C102. See text for a complete description.

The experimental technique has been described in detail previously.[11] The experiment can be thought of in a pump−probe context where the pump pulse is electronically resonant with the solute and we label the pump−probe time delay t. The laser pulse sequence is illustrated in the inset of Figure 2. The probe consists of three electronically nonresonant laser pulses, with the first two time co-incident and the third at a variable time delay labeled τ. The probe measures the time domain Raman response, i.e., a two-point polarizability correlation function, $R_{probe} \propto \langle \alpha(\tau)\, \alpha(0) \rangle_{\rho_{eq}}$. As a point of reference, the probe is analogous to the response measured in optical Kerr effect spectroscopy, or OKE.[12−14] Experiments were performed using our home-built, regeneratively amplified, 1 kHz titanium: sapphire based laser system.[10] The three probe pulses were 38 fs (Gaussian, FWHM) and centered at 800 nm. Pump pulses centered at 400 nm (spectrum shown in Figure 1) were created by frequency doubling the 800 nm pulses in a 100 μm type-I β-BaB_2O_4 crystal and were 35 fs (Gaussian, FWHM) in duration. The 400 nm pump pulses were modulated at half the laser repetition rate, and the probe signal was collected via lock-in detection at the modulated frequency. The result provides a measurement of the change in the probe response as a result of C102 excitation by the pump pulse.

Coumarin 102 was obtained from Exciton, Inc and used as received. Acetonitrile (Pharmco HPLC grade) and water (Millipore) were used without further purification. Solutions of acetonitrile−water binary mixtures at $x_{CH_3CN} = 0.25, 0.50, 0.75$, and 1.0 were used in the experiments. The optical density of the solutions was typically 0.4 at 400 nm corresponding to a C102 concentration of $\sim 1.9 \times 10^{-4}$ M. The solutions were circulated in a 1 mm path length quartz flow cell at a rate of 0.1 mL/s. Absorption spectra were recorded on an Olis Cary 14 spectrometer and are shown in Figure 1.

Figure 2 shows the measured responses for the three binary mixtures and neat acetonitrile at a fixed intrinsic probe delay of $\tau = 110$ fs. The data were fit with basic functional forms subsequently convoluted over the instrument response function and added to the background measured on identical solutions without the C102 present. The background was dominated by an instrument limited feature centered at $t = 0$, and this component of the fit is the origin of the noise apparent on the total fits to the data. The fits are presented as the solid lines in Figure 2. For all solutions the fit included an exponential rise and decay,

$$\Delta R_{probe}(t) = W_r\left[1 - \exp\left(\frac{-t}{t_r}\right)\right] + W_d \exp\left(\frac{-t}{t_d}\right) \qquad (1)$$

where W_r and W_d represent adjustable weights. Equation 1 alone was sufficient to obtain satisfactory fits to the results for $x_{CH_3CN} = 1.0$ and 0.75. However, an additional component with positive amplitude and a minimum of two time scales was required to fit $x_{CH_3CN} = 0.5$ and 0.25. This additional component was fit as a series of two first-order events,

$$\Delta R_{probe}(t) = a(t)A \xrightarrow{t_{AB}^{-1}} b(t)B \xrightarrow{t_{BC}^{-1}} c(t)C \qquad (2)$$

The time dependent coefficients, $a(t) - c(t)$, were restricted to a sum of 1 with the initial condition that $a(t{=}0) = 1$. The response amplitudes, $A-C$, and time constants, t_{AB} and t_{BC}, were adjusted as parameters in the fitting.[15] Optimized fitting parameters for all solutions are listed in Table 1. The individual bare fitting components are plotted in Figure 3.

Previous OKE measurements on acetonitrile−water binary mixtures have indicated that the Raman response in this region is dominated by acetonitrile for all of the compositions presented here.[16] A value of $\tau = 110$ fs is near the maximum of the intermolecular response and is typically associated with librational and translational motions.[9,12] The time dependence of the measurements and fits shown in Figure 2 for $x_{CH_3CN} = 1.0$ and 0.75 are not statistically distinguishable from each other, or from

TABLE 1: Fitting Parameters for the Measured Responses Shown in Figure 2[a]

	dipolar solvation (eq 1)				additional dynamics (eq 2)				
x_{CH_3CN}	t_r (ps)	t_d (ps)	W^r	W^d	t_{AB} (ps)	t_{BC} (ps)	A	B	C
1.00	0.13	35.5	−0.65	−0.35					
0.75	0.13	35.5	−0.65	−0.35					
0.50	0.13	35.5	−0.65	−0.35	0.21	0.81	0.0	0.15	0.25
0.25	0.13	35.5	−0.65	−0.35	0.21	0.80	0.0	0.16	0.49

[a] See eqs 1 and 2 for functional forms and definitions of these parameters.

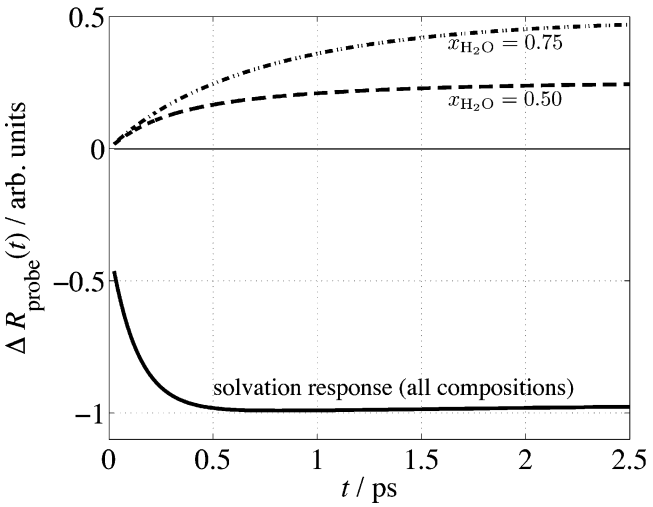

Figure 3. Fits to the change in the third-order nonresonant response. The solid line is the dipolar solvation response used in the fitting of all binary mixtures. The dashed and dash−dot lines are the additional component required to fit the data for $x_{CH_3CN} = 0.50$ and $x_{CH_3CN} = 0.25$, respectively.

our previously reported change in the Raman response that accompanies excitation of C102 in neat acetonitrile.[11] The ultrafast decline in the probe near the peak of the intermolecular response, $t_r = 130$ fs, is a result of the increase in the intermolecular solvent−solute interaction that follows excitation of C102. This is largely the result of electrostatic interactions that change as the dipole moment of C102 increases by ~4 Debye following photoexcitation.[17] The tightening of the intermolecular potential causes a shift in the librational spectrum to higher frequencies and a shift of the collective motions to lower frequencies, analogous to the shift in the intermolecular spectrum measured with increasing density that follows decreasing temperature.[18] The shift of the spectrum due to the tightening of the local solvent environment produces a reduction in the probe response in the middle of the broad intermolecular band, including the response at $\tau = 110$ fs.[11] Although our focus in this letter is on the first few picoseconds after excitation, we note that there is a partial recovery of this response on a time scale of $t_d = 35$ ps, and this includes a contribution from solute rotation. The negative change in the probe response that follows the tightening of the local environment will be referred to here as the dipolar solvation component, represented in the fits by eq 1 and shown in Figure 3. This is a component of the response in all of the solutions, and is the only component necessary to fit the data for $x_{CH_3CN} = 1.0$ and 0.75.

As the water mole fraction is increased above $x_{H_2O} = 0.25$, a new component appears in the transients shown in Figure 2. There is an increase in the signal that follows the rapid initial decrease from the dipolar solvation response. The additional response is represented by eq 2 in the fits, and is shown in Figure 3. We have previously discussed origins for an increase near the peak of the intermolecular response.[15] These involve the opposite shift of the intermolecular spectrum to that described above, and can roughly be associated with a loosening of the solvent environment. One possibility is a reduction of the electrostatic intermolecular solvent−solute interaction. Another possibility is an increase in the kinetic energy of the solvent. This would be analogous to the change in the intermolecular spectrum measured with increasing temperature and concomitant decreasing density.[18] In the absence of an argument to explain a significant reduction of the electrostatic solvent−solute interaction subsequent to the initial dipolar solvation response, we propose that the additional response is the result of an impulsive reactive event in the excited state. A similar increase in the solvent response is produced following ultrafast excited state intramolecular proton transfer.[15]

The agreement between the initial time scale of the additional response, t_{AB} in Table 1, and the previous reports of bond cleavage between excited state C102 and nonaqueous hydrogen bond donors strongly suggests that our observations are the result of impulsive bond cleavage between C102 and water.[3−7] The second time scale, t_{BC} in Table 1, likely reflects the solvent reorganization and kinetic energy transfer that follows the initial impulsive bond disruption. Although these dynamics are consistent with sudden disruption of hydrogen bonding, the water composition required before the additional response becomes significant, $x_{H_2O} > 0.25$, is much larger than one might expect for a large fraction of the C102 solute molecules to be hydrogen bound to a water. To address this apparent inconsistency, we use computer simulations to investigate C102 hydrogen bonding as a function of solvent composition in more detail. The results indicate that the experimentally observed dynamics are correlated with the hydrogen bonding of not one, but rather two, water molecule donors at the carbonyl acceptor of the C102.

Monte Carlo simulations in the isobaric−isothermal ensemble[19] were carried out on C102 in water−acetonitrile binary mixtures. Water and acetonitrile were modeled by the TIP4P and Transferable Potentials for Phase Equilibria (TraPPE) force fields, respectively.[20,21] The TraPPE force field has not yet been extended to include every interaction site on the C102 molecule, and consequently the intermolecular potential was assembled from various sources.[21−24] United-atom models were used for both acetonitrile and C102, and all molecules were constrainted to be rigid. Long-range corrections for the nonbonded Lennard−Jones interactions were used, as well as Ewald sums to account for the electrostatic interactions.[25] The temperature, external pressure, and solvent compositions were set to the experimental conditions ($T = 298$ K, $p = 1$ atm, and $x_{CH_3CN} = 1.00$, 0.75, 0.50, 0.25, 0.00). A total of 801 molecules was used (one C102 and 800 solvents), and four independent simulations were run for each solvent composition, each having about 40 000 Monte Carlo cycles of equilibration and 60 000−80 000 cycles of production. The structure of C102 was optimized with Kohn−Sham density functional theory (DTF)[26] using the B3LYP exchange-correlation functional[27,28] and the 6-31++G(d,p) basis set implimented in Gaussian03.[29] Partial charges were computed for C102 solvated in water using Charge Model 4 (CM4) for the ground electronic state (S_0).[30] The complete details of the force fields are given elsewhere.[31]

TABLE 2: Hydrogen-Bonding Analysis of C102 with H_2O[a]

x_{CH_3CN}	av no. HB	% 0 HB	% 1 HB	% 2 HB	% 3 HB
0.75	0.86	24(8)	66(7)	10(2)	
0.50	1.36	6(1)	56(6)	36(6)	3(2)
0.25	1.70	1(1)	34(3)	57(3)	7(2)
0.00	2.04	1(1)	19(2)	55(2)	25(2)

[a] Standard error of the mean in parentheses.

The combined distance-angular hydrogen-bonding criterion proposed by Wernet and co-workers is used to define a water molecule as bound to a given site on C102.[32] Because the force field used for C102 was a united-atom model with no hydrogen atoms, C102 can only act as a hydrogen bond acceptor for the water molecules. The average number of water molecules hydrogen bonded to the oxygen atom of the C102 carbonyl, and the percentages of hydrogen-bonding configurations containing 1, 2, or 3 waters is shown in Table 2. Interestingly, when the same analysis was applied to the ester oxygen and the tertiary amine, no significant hydrogen bonding was seen at these sites even in pure water.[31] As can be seen in Table 2, in the case of pure water the ground state CM4 charge model predicts just over two water molecules hydrogen bonded to the carbonyl oxygen on average. It seems to be very reasonable to assume that in water rich environments, C102 will accept around 2 hydrogen bonds to water because the carbonyl is fairly polar, contains two lone electron pairs, and has little steric hindrance. The number of hydrogen bound waters to the oxygen in formaldehyde was found to be 2.5 by two different simulations.[33,34] Because of this, the C102 force field with CM4 partial atomic charges seems to be giving reasonable behavior.

Number integrals from the O−O radial distribution function for the C102 carbonyl oxygen to the oxygen in water show that 3.4, 2.1, 1.7, and 1.0 water molecules sit within 3.5 Å of the carbonyl oxygen of C102 for $x_{CH_3CN} = 0.00$, 0.25, 0.50 and 0.75. The number of hydrogen bound water molecules is less than the coordination number due to the possible orientation of the water molecules, but both analyses indicate that the additional dynamics seen in Figure 2 are likely due to the number of C102 molecules participating in multiple hydrogen bonds. In water-rich environments C102 tends to form hydrogen-bonding structures with at least two water molecules, resembling the structures proposed by Topp for the gas-phase association of two water molecules with C153 and 151.[35,36] There is a clear correlation between the amplitude of the measured additional

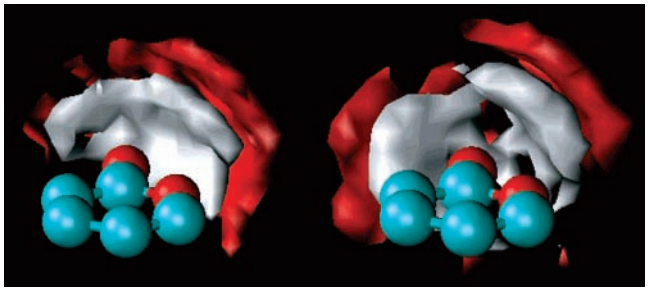

Figure 4. Spatial distribution of the oxygen (red) and hydrogen (white) involved in a hydrogen bond of water with the carbonyl oxygen atom of C102 with $x_{CH_3CN} = 0.50$. The left panel shows the distribution for configurations with one hydrogen bond present, and the right panel shows the distribution for configurations with two hydrogen bonds. The isosurfaces delineate the volume occupied by approximately 80% of all bound molecules. The fragment of the C102 molecule shown in this figure with the ball-and-stick representation is highlighted bold in the complete C102 structure shown in Figure 1.

dynamical component, Figures 2 and 3, and the fraction of C102 molecules with two hydrogen bound water donors at the carbonyl acceptor, Table 2.

Together, the experiments and simulations presented here indicate that hydrogen bond disruption in the C102 excited state is correlated with two bound waters, both as donors at the same carbonyl. This conclusion leads to a description of the dynamics that can simultaneously accommodate both an increase in the hydrogen bond strength calculated by Zhao and Han and disruption of hydrogen bonding.[3−8] Figure 4 compares the cases of C102 participating in hydrogen bonding with one and two water molecules by comparing the single and double hydrogen bond configuration from the MC simulations. As shown, the single hydrogen bond configuration prefers a hydrogen-bonding structure with the water occupying a quarter sphere centered about the lactone group of C102. When a second hydrogen bond forms, the distribution of hydrogen bonds becomes a half sphere about the carbonyl of C102. This shows that in the ground electronic state, removing a water molecule from a C102 participating in hydrogen bonding with two waters is energetically preferable from the α-carbon side of the lactone. The inequivalency of the two hydrogen-bonding sites for C102-water hydrogen bonds suggests that upon electronic excitation, the water participating opposite the α-carbon side is bound more strongly at the expense of the hydrogen bond to the water on the α-carbon side, which is substantially weakened and perhaps broken. An analogous circumstance may exist in the previous reports for nonaqueous hydrogen bonding in poor solvents, where multiple hydrogen-bonding partners are anticipated.[3−7] This offers potential clarification for the previously unexplained hydrogen bond disruption that appeared to be at odds with simulations of the hydrogen-bonding interaction with a single donor.

Acknowledgment. Financial support was provided by the National Science Foundation (CHE-0211894, CHE-0650013, and CTS-0553911), and in part by the MRSEC Program of the NSF under award number DMR-0212302. D.A.B. gratefully acknowledges support from the David and Lucile Packard Foundation. A 3M Foundation Graduate Fellowship (M.J.M.) and a Department of Energy Computational Science Graduate Fellowship (M.J.M.) are gratefully acknowledged. Part of the computer resources were provided by the Minnesota Supercomputing Institute.

References and Notes

(1) Reichardt, C. *Solvents and solvent effects in organic chemistry*, 3rd updated and enlarged ed.; Wiley-VCH: Weinheim, 2003.

(2) Jortner, J., Bixon, M., Eds. *Electron transfer - from isolated molecules to biomolecules*; Advance in Chemistry and Physics; John Wiley and Sons, Inc.: New York, 1999; Vols. 106 and 107.

(3) Chudoba, C.; Nibbering, E. T. J.; Elsaesser, T. *Phys. Rev. Lett.* **1998**, *81*, 3010.

(4) Chudoba, C.; Nibbering, E. T. J.; Elsaesser, T. *J. Phys. Chem. A* **1999**, *103*, 5625.

(5) Nibbering, E. T. J.; Tschirschwitz, F.; Chudoba, C.; Elsaesser, T. *J. Phys. Chem. A* **2000**, *104*, 4236.

(6) Tschirschwitz, F.; Nibbering, E. T. *J. Chem. Phys. Lett.* **1999**, *312*, 169.

(7) Palit, D. K.; Zhang, T.; Kumazaki, S.; Yoshihara, K. *J. Phys. Chem. A* **2003**, *107*, 10798.

(8) Zhao, G.-J.; Han, K.-L. *J. Phys. Chem. A* **2007**, *111*, 2469.

(9) Kumar, P. V.; Maroncelli, M. J. *Chem. Phys.* **1995**, *103*, 3038.

(10) Underwood, D. F.; Blank, D. A. *J. Phys. Chem. A* **2003**, *107*, 956.

(11) Underwood, D. F.; Blank, D. A. *J. Phys. Chem. A* **2005**, *109*, 3295.

(12) Smith, N. A.; Meech, S. R. *Int. Rev. Phys. Chem.* **2002**, *21*, 75.

(13) Cho, M.; Du, M.; Scherer, N. F.; Fleming, G. R.; Mukamel, S. *J. Chem. Phys.* **1993**, *99*, 2410.

(14) McMorrow, D.; Thantu, N.; Melinger, J. S.; Kim, S. K.; Lotshaw, W. T. *J. Phys. Chem.* **1996**, *100*, 10389.

(15) Schmidtke, S. J.; Underwood, D. F.; Blank, D. A. *J. Phys. Chem. A* **2005**, *109*, 7033.

(16) Ernsting, N. P.; Photiadis, G. M.; Hennig, H.; Laurent, T. *J. Phys. Chem. A* **2002**, *106*, 9159.

(17) Cave, R. J.; Castner, J., Edward W. *J. Phys. Chem. A* **2002**, *106*, 12117.

(18) Farrer, R. A.; Loughnane, B. J.; Deschenes, L. A.; Fourkas, J. T. *J. Chem. Phys.* **1997**, *106*, 6901.

(19) McDonald, I. R. *Mol. Phys.* **1972**, *23*, 41.

(20) Jorgensen, W. L.; Chandrasekhar, J.; Madura, J. D.; Impey, R. W.; Klein, M. L. *J. Chem. Phys.* **1983**, *79*, 926.

(21) Wick, C. D.; Stubbs, J. M.; Rai, N.; Siepmann, J. I. *J. Phys. Chem. B* **2005**, *109*, 18974.

(22) Wick, C. D.; Martin, M. G.; Siepmann, J. I. *J. Phys. Chem. B* **2000**, *104*, 8008.

(23) Wick, C. D.; Siepmann, J. I.; Sheth, A. R.; Grant, D. J. W.; Karaborni, S. *Crys. Growth Des.* **2006**, *6*, 1318.

(24) Martin, M. G.; Siepmann, J. I. *J. Phys. Chem. B* **1998**, *102*, 2569.

(25) Frenkel, D.; Smit, B. *Understanding Molecular Simulation: From Algorithms to Applications*; Academic Press: San Diego, CA, 1996.

(26) Kohn, W.; Sham, L. *J. Phys. Rev.* **1965**, *140*, A1133.

(27) Becke, A. D. *J. Chem. Phys.* **1993**, *98*, 5648.

(28) Lee, C.; Yang, W.; Parr, R. G. *Phys. Rev. B* **1988**, *37*, 785.

(29) Frisch, M. J.; Trucks, G. W.; Schlegel, H. B.; Scuseria, G. E.; Robb, M. A.; Cheeseman, J. R.; Montgomery, J. A., Jr.; Vreven, T.; Kudin, K. N.; Burant, J. C.; Millam, J. M.; Iyengar, S. S.; Tomasi, J.; V. B.; Mennucci, B.; Cossi, M.; Scalmani, G.; Rega, N.; Petersson, G. A.; Nakatsuji, H.; Hada, M.; Ehara, M.; Toyota, K.; R. F.; Hasegawa, J.; Ishida, M.; Nakajima, T.; Honda, Y.; Kitao, O.; Nakai, H.; Klene, M.; Li, X.; Knox, J. E.; Hratchian, J. E.; Cross, J. B.; Bakken, V.; Adamo, C.; Jaramillo, J.; Gomperts, R.; Stratmann, R. E.; Yazyev, O.; Austin, A. J.; Cammi, R.; Pomelli, C.; Ochterski, J. W.; Ayala, P. Y.; Morokuma, K.; Voth, G. A.; Salvador, P.; Dannenberg, J. J.; Zakrzewski, V. G.; Dapprich, S.; Daniels, A. D.; Strain, M. C.; Farkas, O.; Malick, D. K.; Rabuck, A. D.; Raghavachari, K.; Foresman, J. B.; Ortiz, J. V.; Cui, Q.; Baboul, A. G.; Clifford, S.; Cioslowski, J.; Stefanov, B. B.; Liu, G.; Liashenko, A.; Piskorz, P.; Komaromi, I.; Martin, R. L.; Fox, D. J.; Keith, T.; Al-Laham, M. A.; Peng, C. Y.; Nanayakkara, A.; Challacombe, M.; Gill, P. M. W.; Johnson, B.; Chen, W.; Wong, M. W.; Gonzalez, C.; Pople, J. A. *Gaussian 03*, revision C.02; Gaussian, Inc.: Wallingford, CT, 2004.

(30) Kelly, C. P.; Cramer, C. J.; Truhlar, D. G. *J. Chem. Theo. Comp.* **2005**, *1*, 1133.

(31) McGrath, M. J. Monte Carlo Simulations of Hydrogen Bonding Fluids. Ph.D. thesis, University of Minnesota, 2007.

(32) Wernet, P.; Nordlund, D.; Bergmann, U.; Cavalleri, M.; Odelius, M.; Ogasawara, H.; Naeslund, L. A.; Hirsch, T. K.; Ojamaee, L.; Glatzel, P.; Pettersson, L. G. M.; Nilsson, A. *Science* **2004**, *304*, 995.

(33) Blair, J. T.; Krogh-Jespersen, K.; Levy, R. M. *J. Am. Chem. Soc.* **1989**, *111*, 6948.

(34) Canuto, S.; Coutinho, K. *Intl. J. Quantum Chem.* **2000**, *77*, 192.

(35) Pryor, B. A.; Palmer, P. M.; Chen, Y.; Topp, M. R. *Chem. Phys. Lett.* **1999**, *299*, 536.

(36) Pryor, B. A.; Palmer, P. M.; Andrews, P. M.; Berger, M. B.; Topp, M. R. *J. Phys. Chem. A* **1998**, *102*, 3284.